

Prompt emission of dipole radiation in nuclear reactions with radioactive beams

C.H. Dasso¹, H. Sofia^{2,a}, and A. Vitturi³¹ ECT* and Dipartimento di Fisica, Università di Trento, Trento, Italy and University of Sevilla, Sevilla, Spain² Departamento de Física, Comisión Nacional de Energía Atómica, Buenos Aires, Argentina³ Dipartimento di Fisica and INFN, Università di Padova, Padova, Italy

Received: 28 March 2001 / Revised version: 29 September 2001

Communicated by P. Schuck

Abstract. Radioactive beams expand considerably the range of reactions with a large charge-to-mass asymmetry between projectile and target that can be probed experimentally. We introduce a simple model to estimate the magnitude and energy distribution of the prompt dipole gamma-emission that takes place while the symmetry is restored during the short contact time. In addition to this pre-equilibrium component we also introduce a procedure to calculate the delayed gamma-emission of statistical character that occurs after thermal equilibration of the compound system—or the binary reaction ejectiles—is reached.

PACS. 21.60.-n Nuclear-structure models and methods – 23.20.Js Multipole matrix elements

1 Introduction

Since the earliest stages in the study of deep-inelastic collisions it has been known that motion in the mass asymmetry degree of freedom is a rather slow process. Thus, how much of the path towards equilibrium can be completed while the densities still overlap becomes an essential ingredient to understand the observed distributions of the mass for the projectile-like and target-like emerging fragments. Relaxation in the charge-to-mass asymmetry degree of freedom is, on the other hand, a much faster process occurring in a time scale comparable to that of the physical contact between projectile and target [1]. Even if the collision leads to fusion, the reshuffling of protons and neutrons that establishes charge-to-mass equilibrium over the entire volume takes place during intervals of time of the order of $\approx 10^{-21}$ s. This scale establishes a qualitative distinction between the prompt emission of γ -radiation and the one that follows thermalization of the highly excited reaction products. In this context, we can equally consider here a fusion reaction, where the source of statistical emission is the resulting compound system, or a deep-inelastic collision leading to two hot emerging fragments which subsequently decay.

As stated previously, the mass drift leaves a clear signature of the process on the experimentally measured mass distributions. Motion along the charge-to-mass degree of freedom may not be that straightforward but can also be traced, insofar as the rapid rearrangement of

charge is accompanied by an emission of dipole radiation that is observable.

Since stable, light systems have $Z/N \approx 1$ one may get the impression that shooting a beam of such nuclei on a medium heavy target ($Z/N \approx 0.65$) should create favorable conditions to trigger a substantial emission of such prompt dipole radiation. The argument that leads to this conclusion is, however, incorrect; what really matters is how much the *absolute* value of the charge $e\delta Z$ that must be shifted around to restore the charge-to-mass balance is. Since normally $\delta Z/Z \ll 1$, the relevant information cannot be extracted from a simple inspection of the ratios Z/N . Reactions with radioactive beams are an altogether different matter, as one can now prepare situations that enforce a larger exchange of protons and neutrons to achieve the overall equilibrium ratio $(Z_P + Z_T)/(N_P + N_T)$. In fact, just by moving the projectile one or two units of charge further away from the stability valley (something that changes little the overall lack of balance between the ratios Z/N for the projectile and target) one can bring about a significant enhancement in the pre-equilibrium radiation yield.

This possibility has been discussed theoretically by several authors [2–4] previously, and experimental efforts have been oriented towards this goal [5–8]. Among the most fundamental approaches it is worth mentioning those that exploit the time dependence of the mean field obtained from solving the BBU equations [4]. It is our opinion that the practical implementation of this technique is not completely free from ambiguities, especially in what concerns the setting up of the initial conditions, aspects

^a e-mail: sofia@tandar.cnea.gov.ar

that may affect its predictive power. The search for a viable alternative to such elaborate calculations provides the motivation for our work. We aim at an operating scheme that —albeit remaining simple— incorporates sufficient physical input to qualify as a useful tool for the interpretation of existing experimental data. In particular, we think also of its possible use in the rapidly expanding field of reactions with radioactive beams, where there is a need for general guidelines that can provide orientation in the design of new experiments.

The organization of the paper is as follows. Section 2 introduces the expressions that we use to estimate the probability for emission of pre-equilibrium dipole radiation and its distribution in energy. We refer here to the specific case of fusion reactions but the formalism applies to the case of deep-inelastic collisions as well. In sect. 3 we complement the radiation spectra thus obtained by adding the statistical emission of dipole photons that takes place in a time-delayed scale. This latter process occurs in conjunction with the evaporation of nucleons and a set of coupled-channel equations that mimics a cascade calculation is implemented. Applications of the scheme are presented in sect. 4 for different systems. The fusion process induced by the reaction $^{40}\text{Ca} + ^{100}\text{Mo}$ at low energies and the deep-inelastic regime in the reaction $^{32}\text{S} + ^{74}\text{Ge}$ are discussed. Concluding remarks close the presentation in sect. 5.

2 The pre-equilibrium part of the γ spectrum

In this section we introduce the expressions used to construct the probability for the emission of prompt dipole radiation and its energy distribution.

One could, in principle, develop a formalism to predict the expected mean frequency of the photons emitted during the fast rearrangement of charge that takes place during the collision time. This would involve a series of assumptions concerning the spatial distribution of the charges in the projectile and target at the point of contact and the nature of the nucleon flow that ensues. However, calculations along these lines are rather complicated and the inevitable uncertainty over the accuracy of the results would not justify the implementation of such an approach. Thus —and in consistency with the stated aim of keeping things simple and reliable— we adopt, instead, a more pragmatic attitude. Since the centroid E_P and spread Γ of the structures in the energy distributions associated with the pre-equilibrium phenomena are put in evidence by the empirical data we will take this information as experimentally given. We then restrict the scope of our study to investigating the existence (and relative magnitude) of these effects in correlation with the mass and charge of the reactants and the excitation energies involved.

The macroscopic specification of the harmonic decay mode requires, as we know, one other parameter besides its energy E_P . We obtain this information from the driving forces that come into play to restore the balance in the charge-to-mass ratio throughout the system. Making use

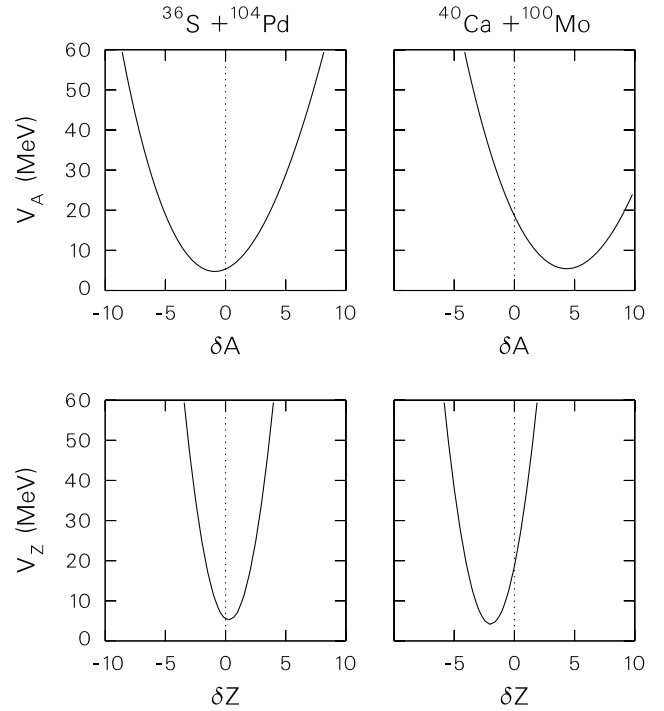


Fig. 1. Cuts of the energy surface $V(\delta A, \delta Z)$ for the systems $^{36}\text{S} + ^{104}\text{Pd}$ (left) and $^{40}\text{Ca} + ^{100}\text{Mo}$ (right). The upper frames show the mass dependence of the potential $V_A(\delta A) \equiv V(\delta A, \delta Z = 0)$, while the lower frames exhibit the charge dependence for $V_Z(\delta Z) \equiv V(\delta A = 0, \delta Z)$. The dotted lines indicate the location of the reference system (the injection point), always defined for $\delta A = \delta Z = 0$. Notice that in the two reactions the same nucleus, ^{140}Sm , is formed. However, the path towards eventual equilibrium in both situations involve a quite different exchange of charge.

of the mass formula

$$M(A, Z)c^2 \approx Zm_Hc^2 + (A - Z)m_n c^2 - a_v A + a_s A^{2/3} + a_c \frac{Z^2}{A^{1/3}} + a_a \frac{(A - 2Z)^2}{A^2},$$

where the parameters a_i are taken from ref. [9], we can approximate the potential energy for two spherical fragments of mass and charge numbers (A_1, Z_1) , (A_2, Z_2) placed at a distance equal to the sum of their radii as

$$V_{\text{ref}} \approx M(A_1, Z_1)c^2 + M(A_2, Z_2)c^2 + \frac{e^2 Z_1 Z_2}{R_1(A_1) + R_2(A_2)}.$$

If a redistribution of nucleons takes place at this contact configuration in such a way that the fragment “one” changes its mass and charge by δA and δZ , the resulting variation in the potential energy can be expressed as

$$V(\delta A, \delta Z) = M(A_1 + \delta A, Z_1 + \delta Z)c^2 + M(A_2 - \delta A, Z_2 - \delta Z)c^2 + \frac{e^2(Z_1 + \delta Z)(Z_2 - \delta Z)}{[R_1(A_1 + \delta A) + R_2(A_2 - \delta A)]} - V_{\text{ref}}.$$

Cuts of this two-dimensional surface in the $(\delta A, \delta Z)$ -plane for $\delta Z = 0$ and $\delta A = 0$ are shown in fig. 1 for the reactions

$^{36}\text{S} + ^{104}\text{Pd}$ and $^{40}\text{Ca} + ^{100}\text{Mo}$. Notice that these are two combinations of reactants that lead to the same nucleus ^{140}Sm . The examples chosen are thus suitable to illustrate different situations that may emerge depending on the initial conditions. To the left, the reaction with sulphur as a projectile, leaves the samarium quite close to the stable isobar. Thus, a relatively minor displacement of charges does, in this case, restore the global charge-to-mass symmetry. One expects that such a reaction will not be accompanied by a substantial emission of pre-equilibrium dipole radiation. To the right, instead, one observes that the injection point (defined always as $\delta A = \delta Z = 0$) forms a composite system farther removed from the stability valley, a condition favorable for the detection of a larger number of prompt emission events.

It is interesting to note that, under this type of scrutiny, the widespread assumption that reactions induced by neutron-rich projectiles and/or targets always favor the prompt emission of dipole radiation appears to be unjustified. Consider, for instance, the reactions $^{48}\text{Ti} + ^{64}\text{Ni}$ and $^{16}\text{O} + ^{98}\text{Mo}$ leading to the formation of $^{114,112}\text{Sn}$. This situation can be examined also in terms of potential surfaces as those shown in fig. 1. An inspection reveals that insofar as the drive towards stability in the charge-to-mass ratio is concerned, the reaction induced by the stable oxygen nucleus places the resulting tin system in an entirely similar condition as the one associated with the neutron-rich nickel and titanium isotopes.

The curvature of the potential energy as a function of δZ for $\delta A = 0$ (relaxation in the charge degree of freedom) yields the restoring force parameter C . With this value and an estimate for the damping constant Γ one can proceed to calculate the total energy radiated or, equivalently, the number of photons emitted by each fusion event. This is done exploiting standard electromagnetic radiation formulas [10], which establish that the number of prompt photons emitted by interval of energy E is given by

$$\frac{dn_{\gamma}^p(E)}{dE} = \frac{2}{3} \frac{1}{(\hbar c)^3} \frac{p_0^2}{\pi} (E_1^2 + \frac{r^2}{4}) \times \frac{E_1^2 E}{[(E - E_1)^2 + \frac{\Gamma^2}{4}] [(E + E_1)^2 + \frac{\Gamma^2}{4}]},$$

where p_0 is the initial value of the dipole moment (determined by the position of the injection point relative to equilibrium) and $E_1 = \sqrt{E_p^2 - \Gamma^2/4}$ is the “shifted” energy of the damped harmonic motion.

In fig. 2 we show the energy distribution of the promptly emitted radiation for the reaction $^{40}\text{Ca} + ^{100}\text{Mo}$. The different curves correspond to different choices for the value of Γ , as indicated in the figure caption. The areas under each curve give the total number of photons n_{γ}^p emitted and put in evidence a sharp dependence of this quantity on the assumed value of the damping.

3 The statistical part of the γ spectrum

We have discussed in the previous section the γ spectrum produced in the early stage of the reaction, namely

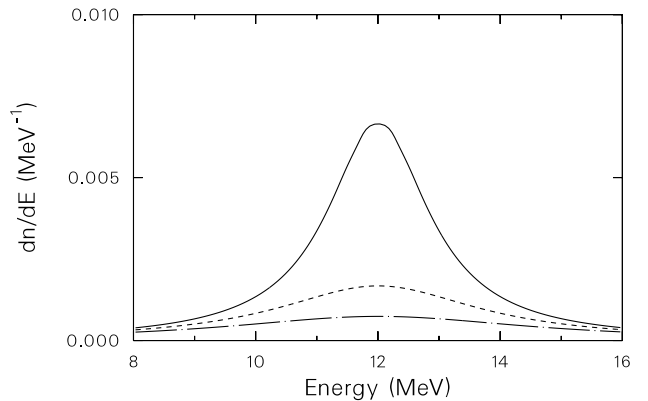


Fig. 2. Energy distribution of the prompt dipole photons for the reaction $^{40}\text{Ca} + ^{100}\text{Mo}$ for different values of the damping width Γ . The full line corresponds to $\Gamma = 2$ MeV, the dashed line to $\Gamma = 4$ MeV and the dash-dotted line to $\Gamma = 6$ MeV. The area under each curve gives the total number of pre-equilibrium photons emitted.

the pre-equilibrium part. In order to compare the predictions of our model with experiment it is necessary to add to this component the contribution of the γ 's that are produced after thermal equilibrium has been reached. In the case of processes leading to fusion, a single compound system is formed, with all the dissipated energy and angular momentum. In the case of deep-inelastic processes one has two separate and independent “hot” systems which share the initial excitation energy and angular momentum. There are available quite sophisticated computer codes to deal with the evaporation cascade processes that follow. In the spirit of this contribution we introduce a simple way to estimate this statistical γ component. To this end we resort to a simple prescription along the lines described, for example, by Brink [2]. Each equilibrated system is assumed to decay by particle and γ emission, and we describe its evolution by simultaneously following in time the average excitation energy $E^*(t)$, the total number $n_n(t)$ of evaporated neutrons and the accumulated number $dn_{\gamma}^d(E, t)/dE$ of delayed γ 's of energy E per unit energy interval up to time t . The usual assumption is made for the corresponding temperature $T(t)$,

$$T(t) = \sqrt{\frac{E^*(t)}{a}},$$

in terms of the level density parameter a , and, under the assumption of a Boltzmann approximation for the density of states, the width for neutron emission $\gamma_{\text{ev}}(t)$ is given within the model by

$$\gamma_{\text{ev}}(t) = \frac{2m}{\hbar^2 c^2 \pi} R^2 T^2(t) e^{-B_n/T(t)},$$

where R and B_n are the system radius and the neutron separation energy. The two decay processes are linked together via the average, time-dependent excitation energy and one just needs to solve the system of coupled

differential equations

$$\frac{dn_n(t)}{dt} = \gamma_{ev}(t),$$

$$\frac{d}{dt} \left(\frac{dn_\gamma^d(E, t)}{dE} \right) = \left(\frac{E}{\pi \hbar c} \right)^2 \sigma_\gamma(E) e^{-E/T(t)}$$

and

$$\frac{dE^*(t)}{dt} = -\frac{dn_n(t)}{dt} (B_n + T(t)) - \int \frac{d}{dt} \left(\frac{dn_\gamma^d(E, t)}{dE} \right) E dE.$$

The cross-section $\sigma_\gamma(E)$ for gamma absorption from the ground state, dominated by the giant dipole resonance with mean energy E_D and width Γ_D , has been fitted with a Lorentzian [11]

$$\sigma_\gamma(E) = \sigma_D \frac{(\Gamma_D E)^2}{(E^2 - E_D^2)^2 + (\Gamma_D E)^2}.$$

Within this scheme, therefore, the inputs for the calculation are the initial excitation energy E_0^* , the average neutron separation energy B_n and the parameters σ_D , E_D and Γ_D for the photoabsorption cross-section in the system considered.

As an example of the results that can be obtained with this set of coupled equations we show, in fig. 3, the gradual build-up of the photon emission spectrum in snapshots timed by the concurrent evaporation of one, two, ... four neutrons. The calculation is for the fusion reaction $^{40}\text{Ca} + ^{100}\text{Mo}$ leading to ^{140}Sm with initial excitation energy $E_0^* = 71$ MeV.

Since details on specific low-lying transitions are ignored, deviations from the predictions of the simple model are expected as the excitation energy decreases and the system approaches its ground state. In particular, as only the contribution of the GDR has been included in the photoabsorption cross-section, this will in particular affect the very low-energy part of the predicted γ spectrum. In addition, in the way we have introduced our prescription there will be a tendency to overestimate the contribution of the delayed γ emission. This is because part of the initial excitation energy is associated with a collective rotation of the system; this component should be subtracted in order to obtain the actual thermal energy available for the de-excitation process.

4 Application to fusion and deep-inelastic reactions

Radioactive beams applied to nuclear reactions has opened the possibility to study nucleus with different Z/N ratios. In order to apply our model, we look to reactions that present pre-equilibrium effects. These effects can be observed by studying the behaviour of the same intermediate system populated via different Z/N asymmetries

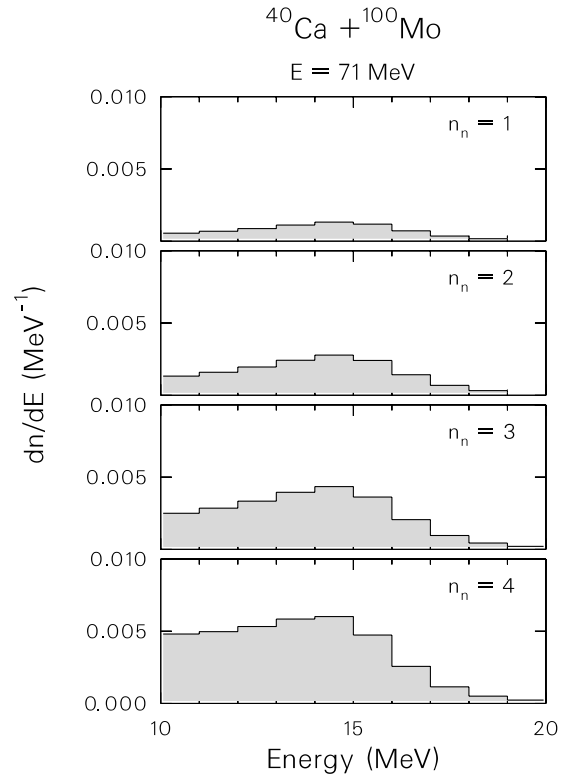


Fig. 3. Energy spectra of the statistical component of the dipole radiation for the reaction $^{40}\text{Ca} + ^{100}\text{Mo}$. Each histogram gives the accumulated distribution of emitted gammas up to the instants of time signaled by the emission of one, two, three and four neutrons (four being the maximum allowed, in average, by the specified value of the initial excitation energy, $E_0^* = 71$ MeV.)

in the entrance channel. These intermediate system could produce a compound nucleus via fusion reactions or fragmentate through a deep-inelastic scattering.

In the case of fusion, we analyze the ^{140}Sm compound nucleus populated via the reactions $^{36}\text{S} + ^{104}\text{Pd}$ and $^{40}\text{Ca} + ^{100}\text{Mo}$ at bombarding energies of 160 and 170 MeV, respectively [5]. The giant dipole resonance decays are very good to study the pre-equilibrium effects due to the different asymmetries of the two reactions. The former reaction, $^{36}\text{S} + ^{104}\text{Pd}$, is almost symmetric and one expects a very small relative strength for the pre-equilibrium dipole radiation. On the other hand, as shown in fig. 1, the $^{40}\text{Ca} + ^{100}\text{Mo}$ reaction has a larger Z/N asymmetry which tends to enhance the fast emission of dipole radiation. In fig. 4 we display, for this system, the prompt, delayed and total components of the dipole radiation energy spectrum. For the pre-equilibrium part, values of $E_P = 12$ MeV and $\Gamma = 4$ MeV were used, as suggested by the experimental data. Parameters for the statistical part of the calculation were $E_D = 15$ MeV, $\Gamma_D = 4.4$ MeV and $\sigma_D = 325$ mb [12]. The prompt component — even in this favorable situation — appears as a minor fraction of the total radiation strength accumulated in the corresponding energy range. Specifically, in this case, it

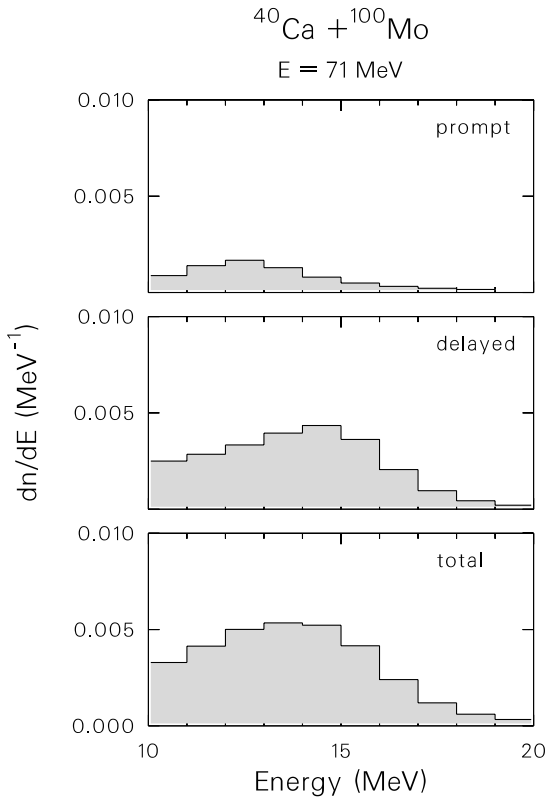


Fig. 4. Same reaction as in fig. 3. In the three frames we compare the energy distribution of the pre-equilibrium photons (top) with that of the delayed or statistical ones (middle) and the combined total for both types of processes (bottom). In this calculation a damping width $\Gamma = 4$ MeV has been used for the evaluation of the prompt component.

contributes between 5 and 20 MeV with about 20% of the total, a level that compares well with the experimental findings of ref. [5], where a 14% value is inferred.

Finally we illustrate in fig. 5 a deep-inelastic situation using the reaction $^{32}\text{S} + ^{74}\text{Ge}$ at 320 MeV of bombarding energy [8]. A total initial excitation energy of 130 MeV, was divided between the two fragments according to their masses. The pre-equilibrium emission was calculated taking $E_P = 12$ MeV and $\Gamma = 2$ MeV. The parameters E_D and Γ_D for the projectile's GDR absorption cross-section were taken to be 24.9 MeV and 4.0 MeV while, for the target, 18.8 MeV and 4.0 MeV. The values chosen of σ_D for each fragment are such that the corresponding TRK sum-rules are exhausted. In addition, a variation of the width Γ_D with temperature was here incorporated, according to the prescription given in refs. [11,13]. With this choice of parameters the pre-equilibrium component turns out to be more comparable in magnitude to the statistical one. This can be better appreciated in the lowest frame of the figure, where the ratio between the total yield and the pure equilibrated component is shown. This ratio reaches at the peak a value 1.8, quite close to the maximum value 1.6 displayed for the same quantity in the experimental measurements of ref. [8].

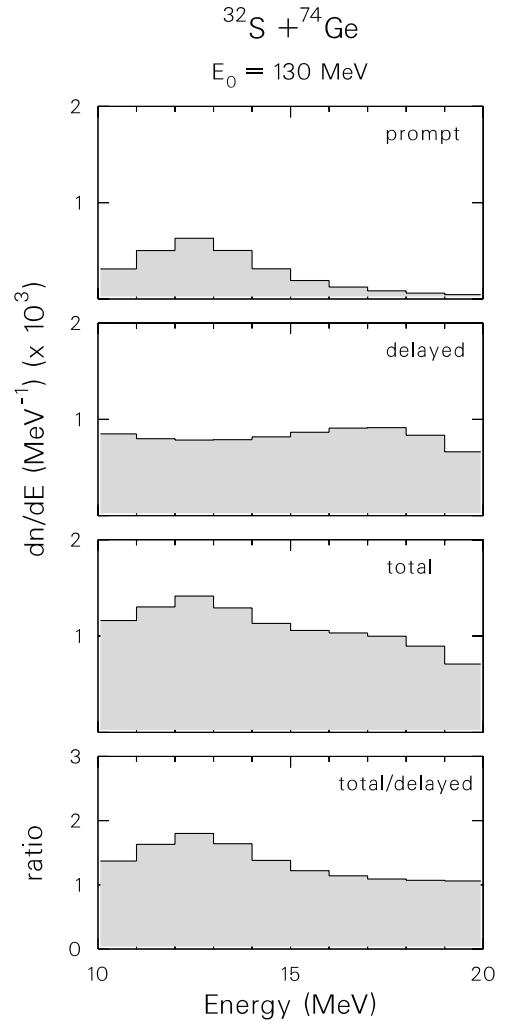


Fig. 5. Same diagram as in fig. 4, for the case of deep-inelastic processes triggered by the reaction $^{32}\text{S} + ^{74}\text{Ge}$. The initial excitation energy of $E_0^* = 130$ MeV is here shared by the emerging fragments according to their masses.

5 Summary

In this paper we study the electric dipole emission induced by reactions with radioactive beams that lead to a large charge-to-mass asymmetry between projectile and target. The reactants can be specifically chosen in this case to generate a significant redistribution of charge before the overall equilibrium in the ratio Z/N is reached. Relaxation in the charge-to-mass asymmetry degree of freedom is a fast process when compared with the thermalization time of the nuclear system (or systems) that result from the collision. This difference of scales reflects in the distinctive experimental signatures that characterize the prompt and delayed components of the photon emission that takes place after the collision has run its course.

In our work we have introduced a simple formalism that incorporates the relevant physical input and provides

a practical tool to analyze experimental data. With this prescription one can, by a straightforward inspection of the gradients of the energy surface defined by the masses and charges of projectile and target, infer the extent to which a given reaction may (or may not) generate a substantial number of prompt-emission events. At the same time, and for general convenience, we have discussed the implementation of a simple coupled-channel scheme that can be used to estimate the delayed emission of dipole radiation. That is, the photons produced after thermal equilibrium is established. These electric transitions occur in competition with the evaporation of particles (mostly neutrons) from the highly excited reaction products. In the case of nuclear fusion it is only the resulting compound nucleus that rids off the energy and angular momentum released in the process; for deep-inelastic processes one considers, instead, the contribution of two independent sources that share the total initial values of these quantities. We note that the results obtained with the suggested alternative are of similar qualitative value as those extracted from modern evaporation codes and much easier to tract.

We have applied the simple model to the fusion process induced by the reaction $^{40}\text{Ca} + ^{100}\text{Mo} \rightarrow ^{140}\text{Sm}$ and to the deep-inelastic regime in the reaction $^{32}\text{S} + ^{74}\text{Ge}$. The results we have obtained show a reasonable agreement with the experimental data.

We thank D. Pierroutsakou and P.F. Bortignon for discussions and suggestions.

References

1. D.A. Bromley (Editor), *Treatise on Heavy Ion Science: Nuclei far from Stability* (Plenum Press, New York, 1989).
2. D.M. Brink, Nucl. Phys. A **482**, 3c (1988).
3. Ph. Chomaz, M. di Toro, A. Smerzi, Nucl. Phys. A **563**, 509 (1993).
4. V. Baran, M. Colonna, M. di Toro, A. Guarnera, A. Smerzi, Nucl. Phys. A **600**, 111 (1996).
5. S. Flibotte, Ph. Chomaz, M. Colonna, M. Cromaz, J. DeGraaf, T.E. Drake, A. Galindo-Uribarri, V.P. Janzen, J. Jonkman, S.W. Marshall, S.M. Mullins, J.M. Nieminen, D.C. Radford, J. L. Rodriguez, J.C. Waddington, D. Ward, J.N. Wilson, Phys. Rev. Lett. **77**, 1448 (1996).
6. M. Sandoli et al., Z. Phys. A **357**, 67 (1997).
7. M. Trotta, A. Boiano, A. De Rosa, G. Inghima, M. La Commara, A. Ordine, D. Pierroutsakou, M. Romoli, M. Sandoli, F. Rizzo, F. Amorini, S. Tudisco, edited by N. Dinh Dang, U. Garg, S. Yamaji, RIKEN Review no. 23 (1999) p. 96.
8. M. Sandoli, A. Boiano, L. Campajola, A. De Rosa, A. D'Onofrio, G. Inghima, M. La Commara, A. Ordine, D. Pierroutsakou, V. Roca, M. Romano, M. Romoli, M. Trotta, F. Rizzo, F. Amorini, S. Tudisco, Eur. Phys. J. A **6**, 275 (1999).
9. A. Bohr, B.R. Mottelson, *Nuclear Structure* (World Scientific, 1998).
10. J.D. Jackson, *Classical Electrodynamics*, 3rd edition (Wiley & Sons Inc., 1998).
11. A. Bracco, F. Camera, J.J. Gaardhoje, B. Herskind, M. Pignanelli, Nucl. Phys. A **519**, 47c (1990).
12. B.L. Berman, F.C. Fultz, Rev. Mod. Phys. **47**, 713 (1975).
13. D. Kusnezov, Y. Alhassid, K.A. Snover, Nucl. Phys. A **649**, 193c (1999).